Probing bilinear R–parity violating supergravity at the LHC

F. de Campos[*]

Departamento de Física e Química, Universidade Estadual Paulista,
Av. Dr. Ariberto Pereira da Cunha, 333, 12516-410, Guaratinguetá – SP, Brazil

O. J. P. Éboli[†]

Instituto de Física, Universidade de São Paulo,
C.P. 66318, 05315-970, São Paulo – SP, Brazil.

M. B. Magro[‡]

Faculdade de Engenharia, Centro Universitário Fundação Santo André,
Av. Príncipe de Gales, 821, 09060-650, Santo André – SP, Brazil.

W. Porod[§]

Institut für Theoretische Physik und Astronomie Universität Würzburg
Am Hubland 97074 Wuerzburg

D. Restrepo[¶]

Instituto de Física, Universidad de Antioquia
A.A. 1226, Medellin, Colombia

M. Hirsch[**] and J. W. F. Valle[††]

AHEP Group, Institut de Física Corpuscular – C.S.I.C./Universitat de València
Edificio Institutos de Paterna, Apt 22085, E–46071 Valencia, Spain
(Dated: February 13, 2013)

We study the collider phenomenology of bilinear R–parity violating supergravity, the simplest effective model for supersymmetric neutrino masses accounting for the current neutrino oscillation data. At the CERN Large Hadron Collider the center–of–mass energy will be high enough to probe directly these models through the search for the superpartners of the Standard Model (SM) particles. We analyze the impact of R–parity violation on the canonical supersymmetry searches – that is, we examine how the decay of the lightest supersymmetric particle (LSP) via bilinear R–parity violating interactions degrades the average expected missing momentum of the reactions and show how this diminishes the reach in the *usual* channels for supersymmetry searches. However, the R–parity violating interactions lead to an enhancement of the final states containing isolated same-sign dileptons and trileptons, compensating the reach loss in the fully inclusive channel. We show how the searches for *displaced vertices* associated to LSP decay substantially increase the coverage in supergravity parameter space, giving the corresponding reaches for two reference luminosities of 10 and 100 fb^{-1} and compare with those of the R–parity conserving minimal supergravity model.

PACS numbers: 12.10.Dm, 12.60.Jv, 14.60.St, 98.80.Cq

[*]Electronic address: camposc@feg.unesp.br
[†]Electronic address: eboli@fma.if.usp.br

February 13, 2013

I. INTRODUCTION

Weak scale supersymmetry (SUSY) represents the most popular approach towards a solution of the hierarchy problem, with the added virtue of being perturbative and accounting for the unification of the gauge coupling constants and the possibility of eventually including gravity [1]. Little is currently known about the detailed mechanism of how SUSY is realized and of how it is broken. Ultimately only experiment can settle this issue. The most popular ansatz *assumes* that R–parity is conserved and that SUSY breaking in a hidden sector is communicated to the observable sector by flavour-blind gravitational interactions. Neither of these assumptions is mandatory, in fact they are both *ad hoc*. Many different mechanisms of supersymmetry breaking can be envisaged [2, 3, 4] and, similarly, the breaking of R–parity [5] can take place in a variety of ways [6, 7, 8].

Here we will adopt only the first part of the conventional ansatz, namely assume transmission of super-symmetry breaking via gravity but relax the R–parity conservation assumption. A specially interesting possibility is that R–parity breaks spontaneously, as a result of the minimization of the scalar Higgs potential [9], very much in the same way as the electroweak symmetry itself breaks. Spontaneous R-parity breaking models are characterized by two types of sneutrino vacuum expectation values (vev) [48], those of right and left-handed sneutrinos, singlets and doublets under SU(3) $\otimes$ SU(2) $\otimes$ U(1) respectively, obeying the "vev-seesaw" relation $v_L v_R \sim h_\nu m_W^2$ where h_ν is the small Yukawa coupling that governs the strength of R–parity violation [9]. Below the scale v_R the effective breaking of R–parity is explicit through bilinear superpotential terms and the corresponding soft supersymmetry breaking terms. For generality and simplicity here we replace the right-handed sneutrino v_R vev by the effective bilinear coupling.

We refer to such simple effective bilinear R–parity breaking (BRpV) picture as BRpV–mSUGRA for short [10] [11]. Here we start directly from the BRpV–mSUGRA model, which has a strong phenomenological motivation, besides simplicity, namely that it provides the most economical effective model for supersymmetric neutrino masses, that successfully accounts for the observed pattern of neutrino masses and mixings [12, 13]. Moreover, it has been shown that, despite the smallness of R–parity violation indicated by the neutrino oscillation data, its effects can be tested and the model falsified at collider experiments [14]. Here we focus on the implications of the model for the first stages of the CERN Large Hadron Collider (LHC).

There have been extensive studies of searches for supersymmetric particles but mainly in the context of models with conserved R parity [15, 16, 17, 18]. So far no direct experimental evidence for SUSY in high energy experiments has been found. With the coming into operation of the LHC searches for R–parity breaking signatures [19, 20, 21, 22, 23] acquire stronger motivation not only by their intrinsic interest, but also because they open the exciting possibility of probing the neutrino oscillation angles at collider experiments [24, 25, 26, 27, 28, 29, 30].

[‡]Electronic address: magro@fma.if.usp.br
[§]Electronic address: porod@ific.uv.es
[¶]Electronic address: restrepo@uv.es
[**]Electronic address: mahirsch@ific.uv.es
[††]Electronic address: valle@ific.uv.es

Previously we have studied the Tevatron potential to search for BRpV–mSUGRA in the multilepton channel [19] as well as in the form of displaced vertices [20]. In this work we provide a quantitative analysis of the phenomenological implications of bilinear R–parity breaking supergravity for the LHC, extending our studies to the new energy range accessible at the LHC and including all constraints from neutrino oscillation physics. Since the effective strength of R–parity violation must be small in order to fit current neutrino oscillation data, our study also constitutes a robustness check of the supergravity parameter reach estimates against the presence of "perturbative" BRpV terms. Supersymmetric particle spectra and production cross sections are expected to be the same as the conventional ones, thanks to the smallness of R–parity violation required by neutrino oscillation data. Similarly, processes such as $b \rightarrow s\gamma$ and g-2 are essentially the same in BRpV–mSUGRA as in mSUGRA and hence the resulting constraints for the latter still hold.

The basic difference between BRpV–mSUGRA and the conventional R-parity conserving mSUGRA scenario is that the lightest supersymmetric particle is no longer stable and it decays, typically inside the detector, consequently modifying the SUSY phenomenology at colliders. This has two important implications:

- the neutralino is no longer a viable dark matter candidate; one needs to implement either an axion-like, gravitino [31, 32, 33, 34] or possibly majoron dark matter scheme [35, 36]. Clearly no "SUSY dark matter" constraint should be applied in these models.

- any SUSY particle can be the lightest one, hence it can be electrically charged. For the case of interest assumed here it means that the parameters that lead to stau-LSP are perfectly viable for the searches, and are indeed included in our analysis.

As far as searches go, the LSP decay implies that the missing transverse momentum of the events gets diminished and, correspondingly, an increase of the multiplicities for jets and/or charged leptons in the final state is expected. Most remarkably, within a large range of BRpV–mSUGRA parameters, the LSP can live long enough to give rise to displaced vertices, opening a new window for its search and study. An interesting phenomenological feature of BRpV not present in generic RPV schemes is that it naturally leads to displaced vertices [49].

In this work we have analyzed in detail the impact of the LSP decay on the potential of the LHC to unravel the existence of supersymmetry in the simplest framework where its breaking is gravitational. To achieve this we start from the same conventional R–parity conserving search channels. We demonstrate that the LHC reach is reduced in the jets and missing transverse momentum channel with respect to the R–parity conserving scenario. Furthermore, we also find that the final state topologies containing isolated charged same-sign di-leptons and trileptons are enhanced, partially compensating the loss of missing momentum brought about by the LSP decay in the all inclusive channel. An especially relevant fact is that the LSP decay can also lead to displaced vertices. We have also investigated the capabilities of the LHC experiments, ATLAS and CMS, to unravel the existence of SUSY with R–parity violation through the search for displaced vertices with a high invariant mass associated to them. In fact, we find that at 100 fb^{-1} the reach in the displaced vertices is typically larger than the one expected in the R–parity conserving scenario, especially at large m_0 values.

II. THE BRPV–MSUGRA MODEL

As already mentioned, here we focus on the phenomenology of the effective theory described by the bilinear R-parity breaking supergravity model in which the MSSM superpotential is supplemented by the

following terms [10]

$$W_{\mathrm{BRpV}} = W_{\mathrm{MSSM}} + \varepsilon_{ab}\epsilon_i \widehat{L}_i^a \widehat{H}_u^b \, , \tag{1}$$

with three extra parameters (ϵ_i), one for each fermion generation. In addition to these bilinear terms, we must also include new soft supersymmetry breaking terms (B_i).

$$V_{\mathrm{soft}} = V_{\mathrm{MSSM}} - \varepsilon_{ab}\left(B_i\epsilon_i \widetilde{L}_i^a H_u^b \right) \, . \tag{2}$$

Taken together, the new terms in the BRpV Lagrangian (the three bilinear ϵ_i and the B_i) lead to the explicit violation of lepton number as well as R–parity. These terms also induce vevs $v_i \equiv v_{Li}$, $i = 1, 2, 3$ for the three left-type sneutrinos. Note, that in general there is no basis where both sets of bilinear R-parity breaking terms can be eliminated at the same time. In the basis where the bilinear terms in the superpotential are rotated away one would obtain a model where the trilinear terms are approximately given by $\lambda_{ijk} = (\epsilon_i/\mu)Y_{E,jk}$ and $\lambda'_{ijk} = (\epsilon_i/\mu)Y_{D,jk}$ [37].

To further specify the model we assume a minimal supergravity framework with universal soft super-symmetry breaking terms at the unification scale. This model contains eleven free parameters, namely

$$m_0 \, , \, m_{1/2} \, , \, \tan\beta \, , \, \mathrm{sign}(\mu) \, , \, A_0 \, , \, \epsilon_i \, , \mathrm{and} \, \Lambda_i \, , \tag{3}$$

where $m_{1/2}$ and m_0 are the common gaugino mass and scalar soft SUSY breaking masses at the unification scale, A_0 is the common trilinear term, and $\tan\beta$ is the ratio between the Higgs field vev's. For convenience, we trade the soft parameters B_i by the "alignment" parameters $\Lambda_i = \epsilon_i v_d + \mu v_i$ which are more directly related to the neutrino–neutralino properties [13].

The bilinear R–parity violating terms give rise to mixing between Standard Model and SUSY particles. For example, in these models neutrinos mix with the neutralinos giving rise to the neutrino masses and mixings after the diagonalization of a $7{\times}7$ mass matrix for neutrinos and neutralinos. At the tree level only one neutrino picks up a mass while the others acquire masses only radiatively [12, 13, 14, 38]. Typically the tree-level scale is the atmospheric scale and, at this approximation, solar neutrino oscillations do not take place. The solar mass splitting is "calculable" and the solar angle acquires a meaning only when loops are included. It has been checked that current neutrino oscillation parameters [39] can be well reproduced provided $|\epsilon_i| \ll |\mu|$, where μ denotes the SUSY bilinear mass parameter [13].

The LSP lifetime depends upon the SUSY spectrum and the R–parity violating parameters. In order to satisfy the neutrino constraints, the R–parity violating interaction must be feeble, thus leading to a lifetime large enough to give rise to displaced vertices [27]. For the sake of illustration, we depict in Figure 1 the $\tilde{\chi}_1^0$ decay length for 100 GeV $< \mathrm{m}_0 <$ 2000 GeV, 300 GeV $< \mathrm{m}_{1/2} <$ 800 GeV, $A_0 = -100$ GeV, $\tan(\beta) = 10$, and $\mathrm{sgn}(\mu) = +1$. We scan randomly all possible BRpV parameter values ϵ_i and Λ_i, and for each SUGRA point in the plot, we accumulate hundreds of solutions compatible with neutrino oscillation data at 3σ level [39]. In this way the top (red) band corresponds to $m_{1/2} = 300$ GeV, and all possible values of ϵ_i and Λ_i compatible with neutrino mixings and squared mass differences at 3σ.

It is important to notice that in our BRpV–mSUGRA scheme, for a given mSUGRA parameter there is a range of variation in the BRpV parameters ϵ_i and Λ_i. While this has no effect in the production cross sections of supersymmetric states, it affects the LSP decay length, as illustrated in Fig. 1. However, the decay length can vary by not more than $\simeq 30\%$ for a fixed value of $m_{1/2}$ over the allowed range of the BRpV parameters, except at small m_0 where light scalars play an important part in the LSP decay.

Apart from generating neutrino masses, neutralino–neutrino mixing also leads to decay of the LSP into Standard Model particles. In scenarios where the lightest neutralino is the LSP its main decays are
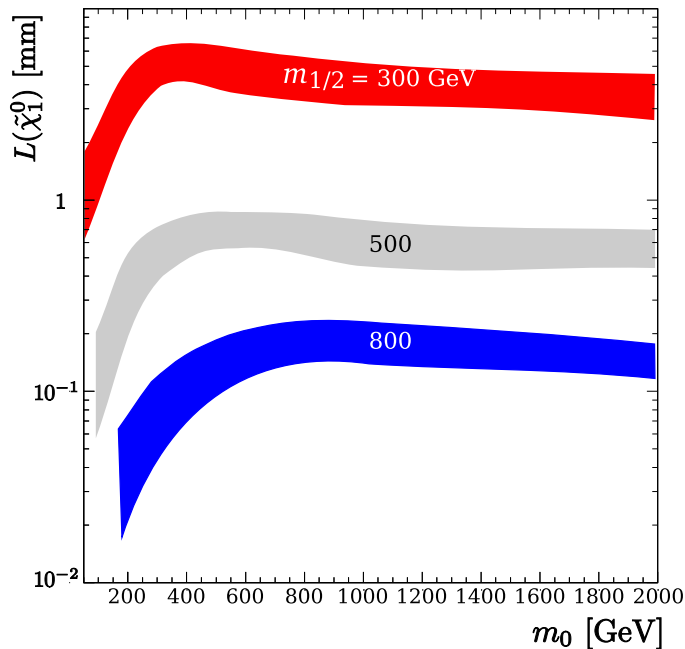
- *leptonic decays:*

FIG. 1: $\tilde{\chi}_1^0$ decay length versus m_0 for $A_0 = -100$ GeV, $\tan\beta = 10$, $\mu > 0$, and several values of $m_{1/2}$. The widths of the three shaded (colored) bands around $m_{1/2} = 300$, 500, 800 GeV correspond to the variation of the BRpV parameters in such a way that the neutrino masses and mixing angles fit the required values [39] within 3σ.

- $\tilde{\chi}_1^0 \to \nu\ell^+\ell^-$ with $\ell = e$, μ denoted by $\ell\ell$;
- $\tilde{\chi}_1^0 \to \nu\tau^+\tau^-$, called $\tau\tau$;
- $\tilde{\chi}_1^0 \to \tau\nu\ell$, called $\tau\ell$.

- *semi-leptonic decays:*

  - $\tilde{\chi}_1^0 \to \nu q\bar{q}$ denoted jj;
  - $\tilde{\chi}_1^0 \to \tau q'\bar{q}$, called τjj;
  - $\tilde{\chi}_1^0 \to \ell q'\bar{q}$, called ℓjj;
  - $\tilde{\chi}_1^0 \to \nu b\bar{b}$, that we denote by bb;
  - $\tilde{\chi}_1^0 \to \nu b\bar{b}$, that we denote by bb;

- *invisible decays:* $\tilde{\chi}_1^0 \to \nu\nu\nu$.

We should mention that many intermediate states contribute to the above decays, like gauge bosons or scalars. Depending on the spectrum, some of these final states can be dominated by 2–body decays. For instance, the decay $\tilde{\chi}_1^0 \to \nu\ell^+\ell^-$ can be dominated by the 2–body $\tilde{\chi}_1^0 \to \nu Z$ followed by $Z \to \ell^+\ell^-$. Another example is the 2–body mode $\tilde{\chi}_1^0 \to \nu h$ with $h \to b\bar{b}$. Consequently we single out the 2–body decays when presenting our results.

Figure 2 presents separately neutralino branching ratios into two-body and three-body decay final states as a function of m_0 for $A_0 = -100$ GeV, $\tan\beta = 10$ and $\mu > 0$. The top panels correspond to a fixed value of $m_{1/2} = 400$ GeV, and the bottom one correspond to $m_{1/2} = 800$ GeV. In the left panels we give branching ratio predictions for optimized ϵ_i and Λ_i BRpV parameter values that reproduce the best neutrino oscillation parameters [39].
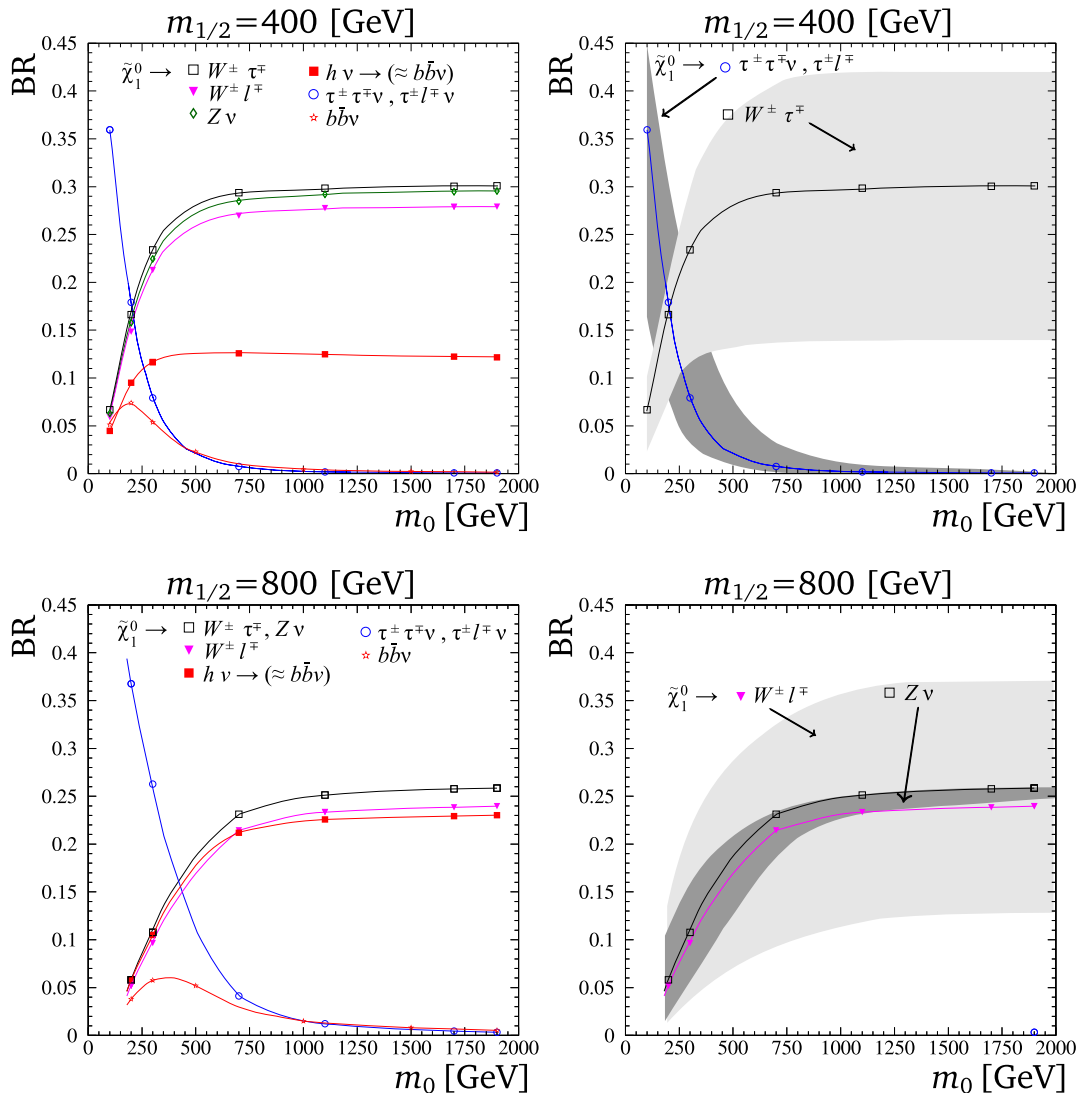
FIG. 2: Lightest neutralino branching ratios as a function of m_0 for $A_0 = -100$ GeV, $\tan\beta = 10$, and $\mu > 0$. In the upper panels we have $m_{1/2} = 400$ GeV while the lower ones the correspond to $m_{1/2} = 800$ GeV. Explanation in text.

Recent neutrino oscillation data from reactors (KamLAND) and accelerators (MINOS) have brought an improved determination of the solar and atmospheric mass squared splittings [39]. On the other hand the solar angle is relatively well determined by current solar neutrino data. In contrast, current uncertainties in the determination of the atmospheric angle remain large and unlikely to improve in the near future. This translates into a large uncertainty in the expectations for the LSP decays into gauge bosons, as illustrated in the right panels in Fig. 2.

The light and dark-shaded grey bands in the right panels in Fig. 2 indicate, as examples, the uncertainties for $\tilde\chi_1^0 \to W^+\tau^-$ and $\tilde\chi_1^0 \to \nu\tau^+\tau^-$ respectively (note that similar uncertainties exist for other channels. For example, $\tilde\chi_1^0 \to W^+\mu^-$ has a similar spread as $\tilde\chi_1^0 \to W^+\tau^-$ but, to avoid an over-crowded plot, we have not displayed). The width of these bands illustrates the effect of varying the BRpV parameters randomly while satisfying the current neutrino oscillation data, especially the atmospheric angle,

at 3σ.

As one can see, for best-chosen values (left panels) the main LSP decay mode at small m_0 is into lepton pairs including a tau, due to light scalar tau exchange. In contrast, for large m_0 values the main decays are into charged lepton (e, μ or τ) accompanied by jets coming from a W.

III. ANALYSIS

In what follows we will describe our two main analysis methods employing first the conventional SUSY search methods and then taking advantage of the displaced vertex technique. As already mentioned all the SUSY particle decays, both R–parity violating as well as R–parity conserving, are calculated using a generalized version of the SPheno code [40][50]. Given a point in SUGRA parameter space, SPheno searches for a set of ϵ_i and Λ_i that leads to neutrino masses and mixings compatible with current neutrino oscillation data. In general, there is a range of R–parity violating parameters that satisfy the above neutrino constraints. As already mentioned, both SUSY spectra and production cross sections are well approximated by the conventional R–parity conserving mSUGRA ones, in view of the smallness of R–parity violation parameters required to fit the neutrino oscillation data. However, for consistency, our version of SPheno calculates spectra and branching ratios including BRpV effects.

We employed PYTHIA version 6.409 [41, 42] to generate the signal and backgrounds, inputting the SPheno output in the SLHA format [43]. Note that we have considered all SUSY production processes in PYTHIA since they all contain two LSP's in the decay chain. Moreover, we have assumed that the detector possesses cells 0.1×0.1 in $\Delta\phi \times \Delta\eta$ and included a Gaussian smearing of the energy with $\Delta(E) = 0.5 \times \sqrt{E}$ (E in GeV). Jets were defined using the subroutine PYCELL with a cone size of $\Delta R = 0.7$. We chose the CTEQ5L parton distribution functions.

A. Standard searches

The LSP decay inside the detector certainly has an important impact in the supersymmetric particle searches at the LHC. For example, visible LSP decays reduce the missing transverse energy leading to a weakening of the standard supersymmetry signals. In order to access the impact of the LSP decay in the usual SUSY searches we analyzed the LHC potential for searching for SUSY in the same final states analyzed in [44], *i.e.*

1. *Inclusive jets and missing transverse momentum* (denoted by (**IN**)): in this case just jets and missing $\not{p}_T$ are taken into account in the analysis;

2. *Zero lepton, jets and missing transverse momentum* (denoted by (**0ℓ**)): here we consider only events presenting jets and missing $\not{p}_T$ without isolated charged leptons ($e^\pm$, $\mu^\pm$);

3. *One lepton, jets and missing transverse momentum* (denoted by (**1ℓ**)): we include in this final state topology only events presenting jets and missing $\not{p}_T$ accompanied by just one isolated charged lepton ($e^\pm$, $\mu^\pm$). Notice that final state τ's contribute to this topology only through their leptonic decays;

4. *Opposite sign lepton pair, jets and missing transverse momentum* (denoted by (**OS**)): this final state is characterized by the presence of jets, missing $\not{p}_T$, and two isolated leptons of opposite charges;

5. *Same sign lepton pair, jets and missing transverse momentum* (denoted by **(SS)**): here we consider only events presenting jets and missing $\not{p}_T$ accompanied by two isolated leptons of the same charge;

6. *Trileptons, jets and missing transverse momentum* (denoted by **(3ℓ)**): we classify in this class events that exhibit jets, missing $\not{p}_T$, and three isolated charged leptons;

7. *Multileptons, jets and missing transverse momentum* (denoted by **(Mℓ)**): this final state presents jets and missing $\not{p}_T$ accompanied by more than three isolated charged leptons.

B. Standard event selection

Our analysis of the topologies defined above follows closely the procedure of [44]. Initially, we applied the acceptance cuts:

AC1 We required at least **two** jets in the event with

$$p_T^j > 50 \text{ GeV} \quad \text{and} \quad |\eta_j| < 3 \,. \tag{4}$$

AC2 In order to suppress a large fraction of the enormous two jet background, we demanded that the transverse sphericity of the event exceeds 0.2

$$S_T > 0.2 \,. \tag{5}$$

AC3 To reduce the background stemming from mismeasured jets, the missing transverse momentum should not be aligned with any jet. Therefore, we imposed that the azimuthal angle ($\Delta\varphi$) between the jets and the missing momentum must comply with

$$\frac{\pi}{6} \leq \Delta\varphi \leq \frac{\pi}{2} \,. \tag{6}$$

In the studies of the different final state topologies we used a floating cut E_T^c designed to give some optimization of the cuts over the parameter space [44]. We considered $E_T^c = 200, 300, 400,$ and 500 GeV. Given one value of E_T^c, we required for all final states that

$$p_T^{1,2} > E_T^c \quad \text{and} \quad \not{p}_T > E_T^c \tag{7}$$

where $p_T^{1,2}$ stand for the transverse momenta of the two hardest jets. These are the only cuts applied for the **IN** topology in addition to **AC1**–**AC3**. Certainly, we could improve the reach in this channel, however, this is beyond the scope of our analysis that aims to access the impact of the LSP decay on the usual SUSY signals.

For the **0ℓ** topology we further veto the presence of isolated leptons with

$$p_T^\ell > 10 \text{ GeV} \quad \text{and} \quad |\eta_\ell| < 2.5 \,. \tag{8}$$

A charged lepton is considered isolated if the energy deposited in a cone of $\Delta R < 0.3$ around its direction is smaller than 5 GeV.

The final state **1ℓ** is obtained imposing (7) and requiring the presence of only one isolated lepton satisfying

$$p_T^\ell > 20 \text{ GeV} \quad \text{and} \quad |\eta_\ell| < 2.5 \,. \tag{9}$$

Aiming the reduction of the potentially large W background, we further imposed that the transverse mass cut

$$m_T(\not{p}_T, p_T^\ell) > 100 \text{ GeV} . \tag{10}$$

The **OS** (**SS**) signal events satisfy (7) and exhibit two isolated leptons with opposite (same) charge. The hardest isolated lepton must have

$$p_T^\ell > 20 \text{ GeV} \quad \text{and} \quad |\eta_\ell| < 2.5 . \tag{11}$$

while the second lepton complies with (8).

Trilepton events ($\mathbf{3\ell}$) must pass the cuts (7) and present three isolated leptons with the hardest one satisfying (11) and the other two respecting (8). Analogously, multilepton events $\mathbf{M\ell}$ are obtained adding one or more isolated lepton to the last topology passing (8).

C.   Standard backgrounds

The main standard model backgrounds for the supersymmetry discovery are

- QCD processes $pp \to jjX$ which have the highest cross section for small values of E_T^c;

- $t\bar{t}$ production that leads to final states $WWbb$ which can lead to many of the final state topologies analyzed here.

- weak gauge boson production in association with jets, denoted by Wj and Zj;

- production of electroweak gauge boson pairs VV with $V = Z$ or W;

- Single top production. Here, we did not include the gluon-W fusion contribution since it is not available in PYTHIA.

We depict in Figure 3 the size and composition of the main SM backgrounds as a function of E_T^c for SUSY searches. Certainly the SM background for the fully inclusive signal (**IN**) is the largest one. For $E_T^c \simeq 100$ GeV it receives a large contribution from QCD processes leading to light quarks and gluon, however, this background decays rapidly with the increase of E_T^c. The main backgrounds for the **IN** topology are $t\bar{t}$ pair production followed by Wj and Zj productions. At this point, it is important to keep in mind that PYTHIA and ISAJET predictions may differ by large factors since they have different hypothesis in the fragmentation process, making difficult the comparison of our results with the ones in reference [44]. For this reason and in order to have a consistent calculation of signal and backgrounds we have redone all background calculations, instead of using the results of this reference.

The $\mathbf{0\ell}$ final state receives a SM backgrounds similar in size and composition to the **IN** topology, therefore, we do not show the results for this case. We can see from Figure 3 that the bulk of the SM background to the $\mathbf{1\ell}$ topology originates from $t\bar{t}$ and Wj production over the entire E_T^c range. The SM background for the **OS** background is sizeable for $E_T^c \lesssim 400$ GeV and it is also dominated by the ubiquitous $t\bar{t}$ production as shown in Figure 3. The **SS** background receives its largest contribution from $t\bar{t}$ pair production with one of them coming from the semi-leptonic b decay, however, it is much smaller than the previous ones and negligible for $E_T^c \gtrsim 200$ GeV. Furthermore, we verified that the Standard Model processes leading to three or more isolated leptons are strongly suppressed, so that the searches are basically background free for the E_T^c range considered in this paper.
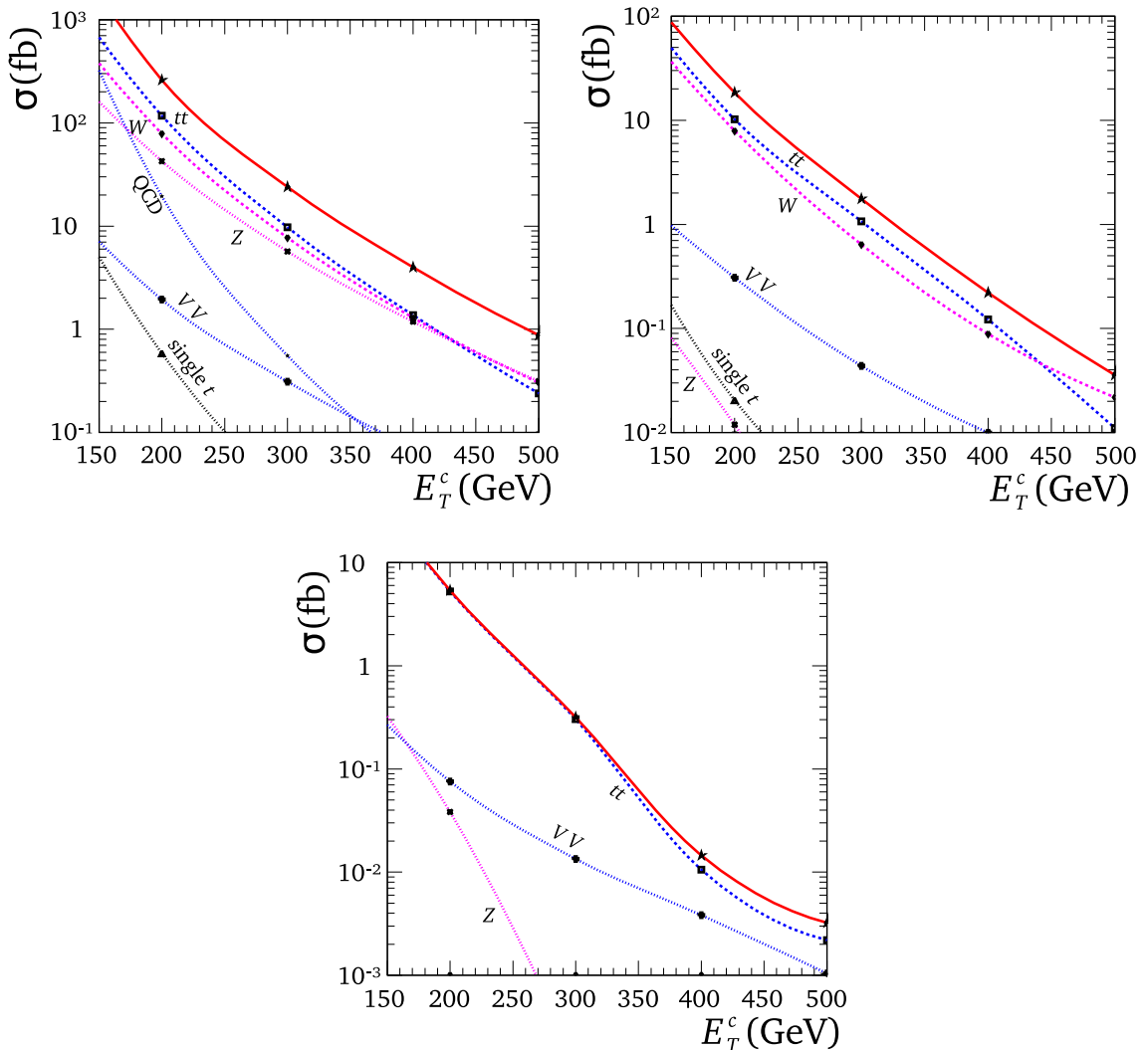
FIG. 3: Composition of the inclusive (top left panel), one lepton (top right panel), opposite sign (lower panel) backgrounds. The top (red) solid lines stands for the total backgrounds while the blue dashed line corresponds to the $t\bar{t}$ background, the magenta dashed lines corresponds to Wj, and the magenta dotted lines stands for the Zj process. The QCD background is represented by the dotted blue line while the dotted black lines stands for the single top production and VV is represented by the lower dotted blue line at small E_T^c.

D. Displaced vertex analysis

Many of the lightest neutralino decay modes presented in Section II can be reconstructed by ATLAS and CMS. We concentrated our analysis on the $\ell\ell$, jj, τjj, bb, $\tau\tau$, and $\tau\ell$ modes. We did not try to fully identify these decays modes because we are only interested in the possible detection of the displaced vertices and not on the further information that can be obtained from them; this analysis will be the subject of another work [45]. For instance, in the decays containing τ's, we kept only the one– and three–prong decays, while we did not study strategies to differentiate the bb from jj modes. In order to assure an almost background free search, we required two reconstructed displaced vertices for each event that pass the requirements presented below.

In our analysis we assumed a toy detector based on ATLAS technical proposal [46]. In order to be

sure that the LSP decayed away from the primary vertex, we required its decay vertex to be outside an ellipsoid

$$\left(\frac{x}{\delta_{xy}}\right)^2 + \left(\frac{y}{\delta_{xy}}\right)^2 + \left(\frac{z}{\delta_z}\right)^2 = 1 \,,$$

where the z-axis is along the beam direction. We were conservative on the choice of the size of axis of the ellipsoid demanding them to be five times the ATLAS expected errors in each direction – that is, $\delta_{xy} = 20 \ \mu$m and $\delta_z = 500 \ \mu$m. We further required that the LSP decay vertex must be inside the pixel inner detector, *i.e.* within a radius of 550 mm and z–axis length of 800 mm. Moreover, to guarantee a high efficiency in the reconstruction of the displaced vertices without a full detector simulation, we restricted our analysis to reconstructed vertex with pseudo-rapidities $|\eta| < 2.5$.

In LSP decays containing τ's or b quarks, there might be additional displaced vertices present further away from the interaction point. Therefore, to reconstruct the LSP decay vertices we required that all visible tracks coming from lightest neutralino decay cascade must cross a sphere of 10 μm around the LSP vertex.

Relatively long lived SM particles, like τ's or B's, can also give rise to displaced vertices as well. However, the Standard Model physics background can be eliminated by requiring that the set of tracks defining a displaced vertex must have an invariant mass larger than 20 GeV. This way the displaced vertex signal passing all the above cuts is essentially background free, except for possible instrument backgrounds which are beyond the scope of this analysis.

At this point we must make sure that the events presenting LSP displaced vertices pass at least of the triggers to guarantee that they will be properly recorded. In order to mimic the triggers used by the LHC collaborations, we accept events passing at least one of the following requirements:

- the event has one isolated electron with $p_T > 20$ GeV and $|\eta| < 2.5$;

- the event has one isolated muon with $p_T > 6$ GeV and $|\eta| < 2.5$;

- the event has two isolated electrons with $p_T > 15$ GeV;

- the event has one jet with $p_T > 100$ GeV;

- the event has missing transversal energy in excess of 100 GeV.

IV.   RESULTS

A.   Standard Analysis

We estimated the SUSY discovery potential of the LHC in the **IN**, **0ℓ**, **1ℓ**, **3ℓ**, **Mℓ**, **OS**, and **SS** channels. We analyzed each channel independently, not trying to combine the outcomes of the different final state topologies. Certainly combining different topologies enhances the LHC reach for SUSY. For the sake of definiteness we defined that a point in the parameter space of our model can be observed in a given channel if there is a choice of E_T^c for which either the signal leads to 5σ departure from the background expectation, where this is not vanishing, or 5 events in regions where the SM background vanishes. We present our results in the $m_{1/2} \otimes m_0$ plane for $\tan\beta = 10$, $\mu > 0$, $A_0 = -100$ GeV, and integrated luminosities of 10 and 100 fb^{-1}.

We depict in Figure 4 the LHC discovery potential in the inclusive (left panel) and one lepton (right panel) channels assuming R–parity conservation as well as bilinear R–parity violation for an integrated

luminosity of 10 fb^{-1}; the results for 100 fb^{-1} are shown in Figure 5. Current direct search limits coming from LEP and Tevatron do not appear in this plot since these constrain lower values of $m_{1/2}$ than the ones displayed, highlighting the increased coverage of the LHC. From the left panel of Fig. 4 one can see how bilinear R–parity violation reduces the reach in the inclusive channel for a given value of m_0 with the signal depletion growing as m_0 increases. Basically, the decay of the LSP in BRpV–mSUGRA reduces the available missing transverse energy making it harder for the signal to pass the cuts, and consequently, stands out from the SM background. This effect is specially important at moderate and high m_0 where the fraction of decays producing neutrinos diminishes; see Fig. 2. Moreover, the shaded area indicates the region where the stau is the LSP. As already discussed, this region is excluded if R–parity is conserved but not in our BRpV–mSUGRA model. We note that the inclusive signal is rather strong in this area.
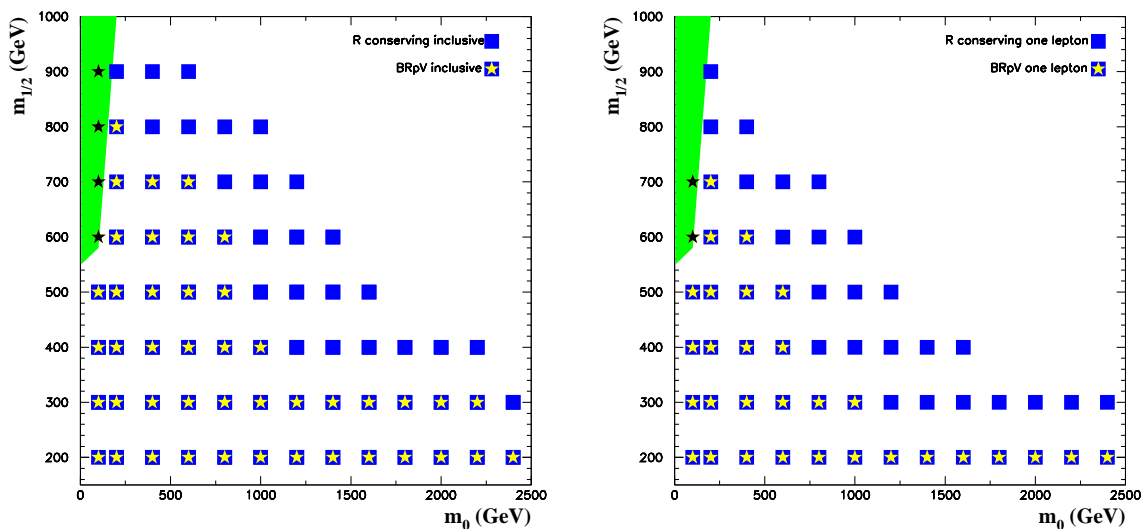

FIG. 4: LHC discovery reach in the inclusive channel (left panel) and in the one lepton channel (right panel). We assumed $\tan\beta = 10$, $\mu > 0$, $A_0 = -100$ GeV, and an integrated luminosity of 10 fb^{-1}. The points leading to visible signal at the LHC are marked by a square for (R-parity-conserving) mSUGRA and by a star for the BRpV–mSUGRA case. The (green) shaded area indicates the region where the stau is the LSP. Points already excluded by LEP and Tevatron searches lie below the $m_{1/2}$ values depicted in this figure.

The reach in the 1ℓ channel is also presented in Fig. 4, right panel, for both cases, with and without R–parity conservation. Clearly from Fig. 4 one can see that, as expected, the reach in this channel is smaller than the one in the inclusive channel with or without R–parity conservation since it diminishes as the slepton masses (m_0) increase. In this channel, the suppression of the signal is larger than the inclusive case when the R–parity violating interactions are present, being visible only at small m_0 ($m_{1/2}$) in the BRpV scenario. This suppression of the one–lepton BRpV signal is due to the reduction of the missing transverse energy at large m_0, while at small m_0 it originates from the production of further leptons in the LSP decay as well. Remember that in this channel we require one and only one isolated charged lepton.

The effect of a larger data sample can be seen in Fig. 5 where we assumed an integrated luminosity of 100 fb^{-1}. The presence of BRpV reduces the signal reach in the inclusive and one-lepton channels when compared to the R–parity conserving case. Moreover, at small and moderate m_0 the inclusive and
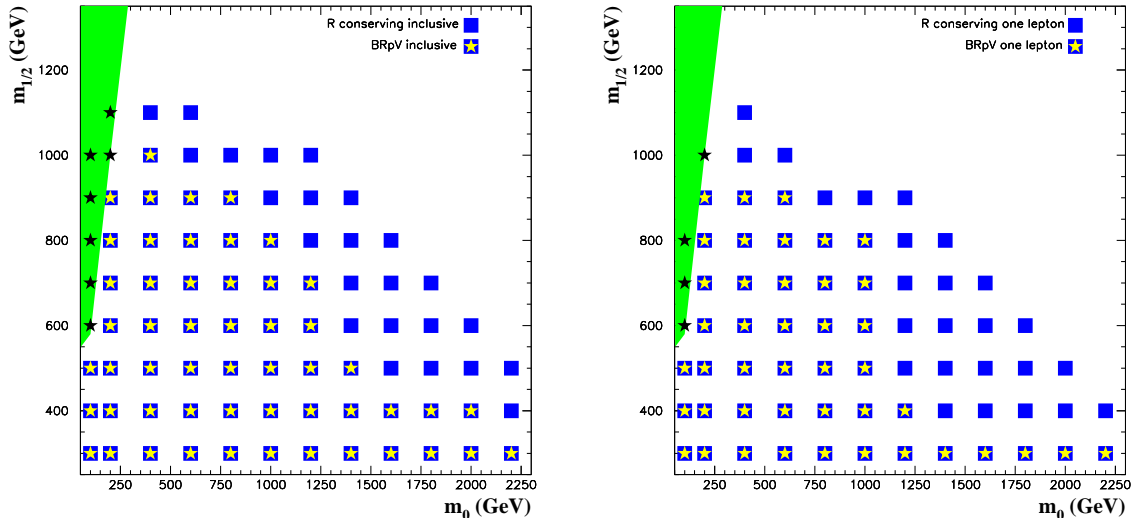
FIG. 5: Same as Fig. 4 but for an integrated luminosity of 100 fb^{-1}.

one-lepton channels lead to similar reach in our BRpV model, however, the inclusive signal has a larger reach for $m_0 \gtrsim 1$ TeV.

In Figures 6 and 7 we present the LHC discovery potential in the opposite (**OS**) and same-sign (**SS**) di-lepton signals (**OS** (left) and **SS** (right)) with/without R–parity conservation for integrated luminosities of 10 and 100 fb^{-1} respectively. Clearly, the presence of R–parity violation extends the LHC reach in this channel at small m_0 with respect to the R–parity conserving scenario. On the other hand the coverage at large m_0 is similar in both cases. Again, this extended reach in the BRpV case is due to the presence of leptons coming from the LSP decay mediated by light sleptons. In the BRpV scenario the **SS** channel provides the largest reach at moderate and large m_0 improving the discovery potential while its reach is similar to the all inclusive channel for BRpV at small m_0. The effect of having a larger data sample, for instance 100 fb^{-1}, is shown in Fig. 7, where we can see that the **SS** signal is more suitable than the fully inclusive signal to search for BRpV models at large m_0.

Figs. 8 and 9 display the LHC reach in the three– (left panel) and multilepton (right–panel) channels with/without R–parity conservation for integrated luminosities of 10 and 100 fb^{-1}, respectively. The discovery potential in these channels is rather limited in the R–parity conserving scenario and it is enhanced when we add the BRpV interactions. It is interesting to notice that the poor reach of the **Mℓ** topology at small $m_{1/2}$ ($\lesssim 200$ GeV) for an integrated luminosity of 10 fb^{-1} is due to the rather hard values of E_T^c used in our analysis. Allowing $E_T^c = 100$ GeV leads to a clear **Mℓ** at small $m_{1/2}$.

For low integrated luminosities (10 fb^{-1}), the **3ℓ** reach is smaller than that of the inclusive channel at small and moderate m_0, however, it leads to a larger coverage at large m_0 in BRpV models. This situation changes drastically at higher luminosities with the trilepton signal becoming by far the main channel for the search of supersymmetry with BRpV. The multilepton channel also becomes very important, being the channel with the second largest reach.

In brief, the decay of the lightest neutralino has an impact of reducing the LHC reach for supersymmetry when we take into account only the main all inclusive channel. Notwithstanding, the new BRpV interactions lead to a substantial increase in the final states containing isolated charged leptons, specially for pairs of same sign leptons and trileptons, compensating the losses in the inclusive channel. If supersymmetry is discovered in a set of the topologies discussed above it must be a rather straightforward
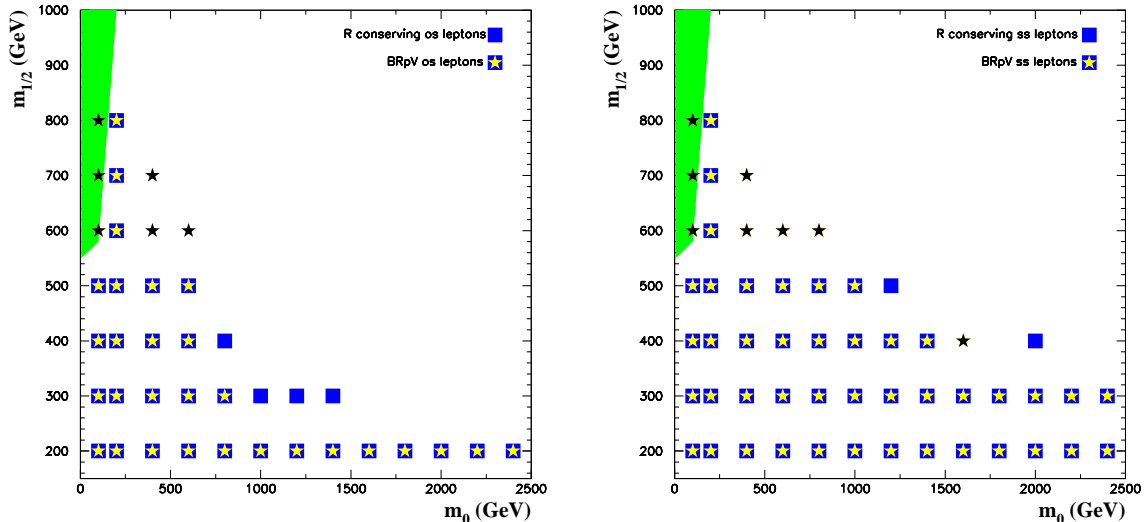
FIG. 6: LHC discovery reach using opposite sign leptons (left panel) and same sign leptons (right panel) for the parameters used in Fig. 4.
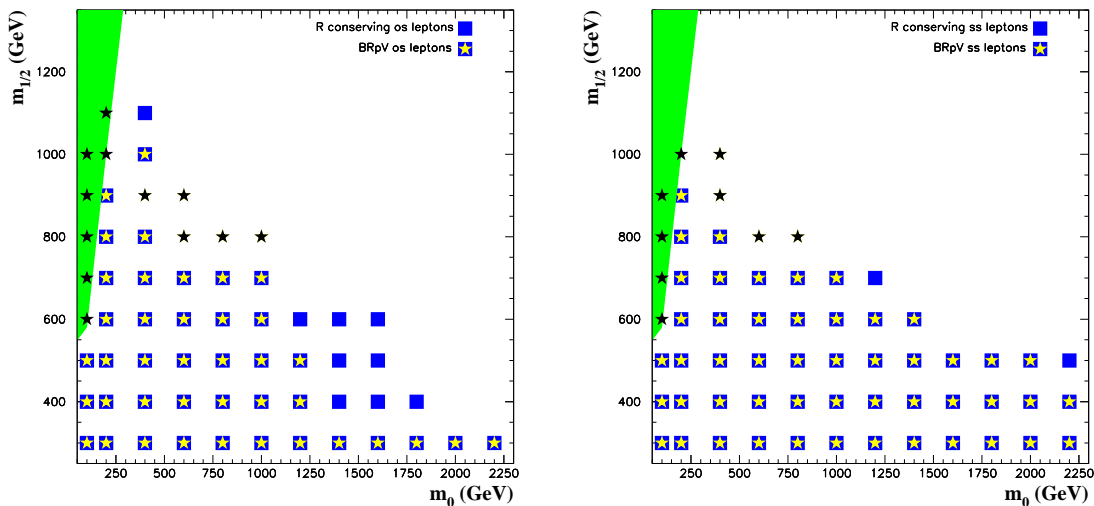

FIG. 7: Same as Fig. 6 but for an integrated luminosity of 100 fb^{-1}.

job to establish the presence of R–parity violating interactions. Now, we turn our attention to another key characteristic feature of our BRpV–mSUGRA model, namely, the emergence of displaced vertices associated to the LSP decay.

B. Displaced Vertices Analysis

Following the criteria previously used to define that a signal can be observed in the canonical supersymmetry topologies, we have searched for points of the parameter space presenting 5 or more identified pairs of displaced vertices for integrated luminosities of 10 and 100 fb^{-1}, assuming that there is no SM background for this search. Our results for the LHC discovery reach in the displaced vertex channel are
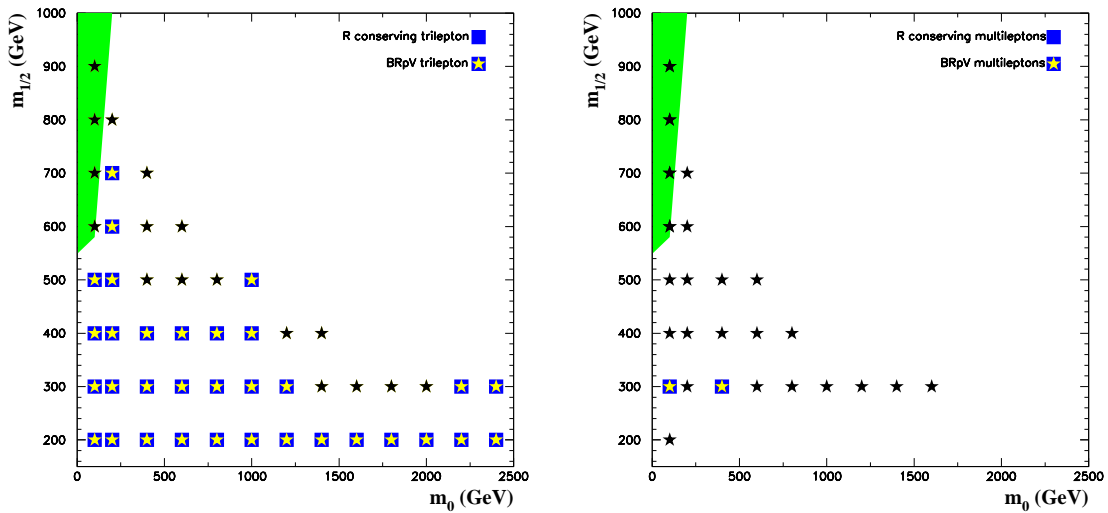
FIG. 8: LHC discovery potential in the three lepton channel (left panel) and the multilepton one (right panel) for the parameters used in Fig. 4.
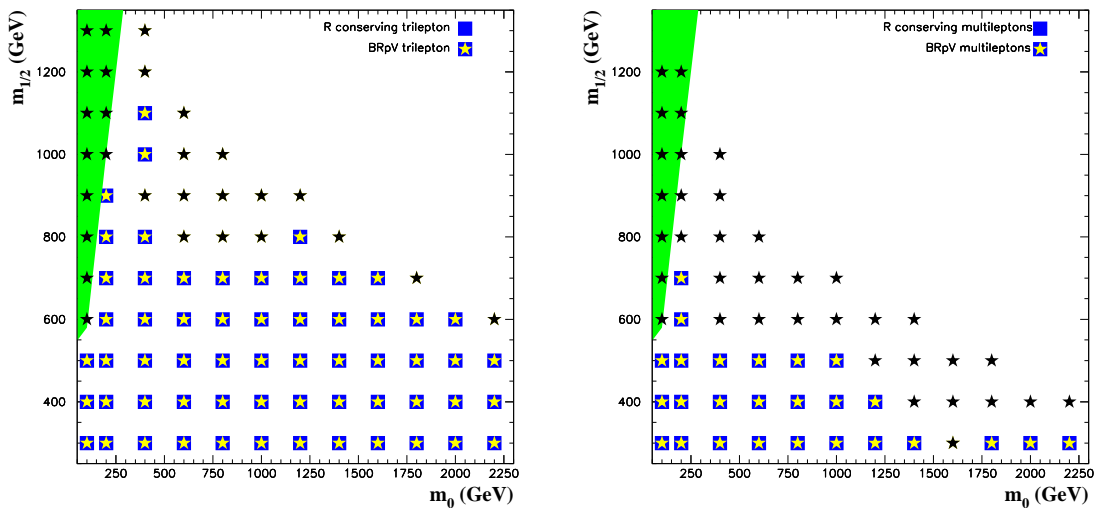

FIG. 9: Same as Fig. 8 but for an integrated luminosity of 100 fb^{-1}.

also shown in the $m_0 \otimes m_{1/2}$ plane for $\tan\beta = 10$, $\mu > 0$ and $A_0 = -100$ GeV.

In Figure 10 we present the displaced vertex reach. As one can see from this figure, the LHC will be able to look for the displaced vertex signal up to $m_{1/2} \sim 800$ (1000) GeV ($m_{\chi_1^0} \sim 340$ (430) GeV) for a large range of m_0 values and an integrated luminosity of 10 (100) fb^{-1}. Notice that the reach in this channel is rather independent of m_0 as expected from Fig. 1. Moreover, this signal for BRpV–mSUGRA disappears in the region where the stau is the LSP due to its rather short lifetime. It is interesting to compare these results with ones obtained in the canonical search channels. The displaced vertex signal provides the largest reach at moderate and large m_0, being more important that the **IN**, **3ℓ** and **Mℓ** topologies. Notwithstanding its good reach at small m_0, it is not the main search channel in this range. Certainly, the combination of the different final state topologies will help us to pinpoint the properties of the model. Furthermore, we should not forget that the discovery of high invariant mass displaced vertices
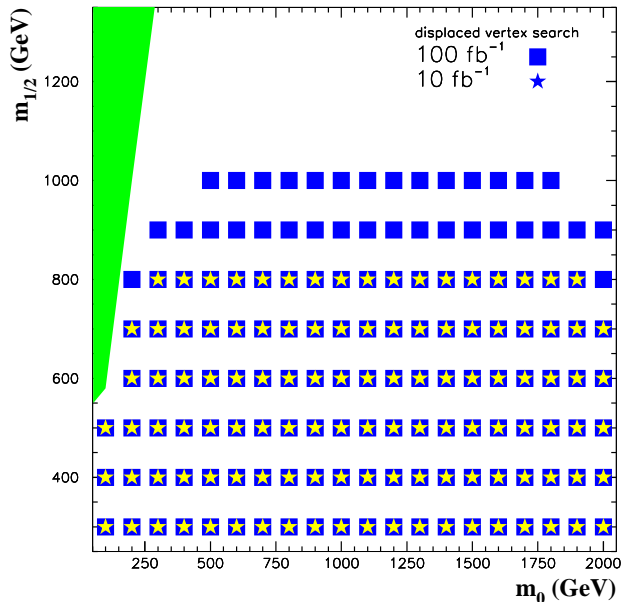
FIG. 10: Discovery reach for displaced vertices channel in the $m_0 \otimes m_{1/2}$ plane for $\tan\beta = 10$, $\mu > 0$, $A_0 = -100$ GeV. The stars (squares) stand for points where there are more than 5 displaced vertex signal events for an integrated luminosity of 10 (100) fb^{-1}. The marked grey (green) area on the left upper corner is the region where the stau is the LSP and the displaced vertex signal disappears. Points already excluded by LEP and Tevatron searches are below the $m_{1/2}$ values depicted in this figure.

allow us to study directly the LSP such as its mass and branching ratios. Moreover, we verified that displaced vertices possess a larger reach than the standard search channels not only at large m_0, but also at large $m_{1/2}$. We expect that for larger values of $\tan\beta$ the reach in the displaced vertex analysis will be even better

Since the LHCb experiment has excellent vertex capabilities, it is natural to conclude that the LHCb can also play an important part in the displaced vertex search for supersymmetry, at least in the first stages of LHC operation, *i.e.* when the accumulated luminosity is rather small [45].

V. CONCLUSIONS

We have considered bilinear R–parity violating supergravity, the simplest effective model for the super-symmetric origin of neutrino masses, reproducing the current neutrino oscillation data. We have given a detailed analysis of the impact of R–parity violation on the standard supersymmetry searches. We have examined how the LSP decays via bilinear R–parity violating interactions degrade the average expected missing momentum in the reactions and shown how this diminishes the reach in the main *canonical* SUSY search channel that is the all inclusive topology. However we have seen how this can be overcompensated by the coverage obtained through the search for final states containing isolated charged leptons, specially the trilepton signal. Moreover, we can also search for displaced LSP decays which can further increase the LHC reach for SUSY. We present the resulting reach in supergravity parameter space for two reference luminosities of 10 & 100 fb^{-1}.

In the first stages of LHC operation, when the accumulated luminosity is rather small, we stress that

a displaced-vertex analysis by the LHCb collaboration can play an important role in probing bilinear R–parity violating supergravity. With enough luminosity to be collected in subsequent stages of operation, the challenge will be to analyze the detailed nature of the LSP decays as a test of the neutrino mixing angles measured in oscillation experiments. We plan to turn to these issues elsewhere.

Acknowledgments

[1] S. P. Martin, (1997), hep-ph/9709356.

[2] A. Brignole, L. E. Ibañez, and C. Muñoz, Nucl. Phys. **B422**, 125 (1994), hep-ph/9308271 Erratum-ibid.B436, 747 (1995).

[3] L. Randall and R. Sundrum, Nucl. Phys. **B557**, 79 (1999), hep-th/9810155.

[4] G. F. Giudice, M. A. Luty, H. Murayama, and R. Rattazzi, JHEP **12**, 027 (1998), hep-ph/9810442.

[5] P. Fayet and S. Ferrara, Phys. Rept. **32**, 249 (1977).

[6] L. J. Hall and M. Suzuki, Nucl. Phys. **B231**, 419 (1984).

[7] G. G. Ross and J. W. F. Valle, Phys. Lett. **B151**, 375 (1985).

[8] J. R. Ellis and et al., Phys. Lett. **B150**, 142 (1985).

[9] A. Masiero and J. W. F. Valle, Phys. Lett. **B251**, 273 (1990); J. C. Romão, C. A. Santos, and J. W. F. Valle, Phys. Lett. **B288**, 311 (1992); J. C. Romão, A. Ioannisian, and J. W. F. Valle, Phys. Rev. **D55**, 427 (1997), hep-ph/9607401.

[10] M. A. Díaz, J. C. Romão, and J. W. F. Valle, Nucl. Phys. **B524**, 23 (1998), hep-ph/9706315.

[11] E. J. Chun, S. K. Kang, C. W. Kim, and U. W. Lee, Nucl. Phys. **B544**, 89 (1999); D. E. Kaplan and A. E. Nelson, JHEP **01**, 033 (2000); F. Takayama and M. Yamaguchi, Phys. Lett. **B476**, 116 (2000); T. Banks, Y. Grossman, E. Nardi, and Y. Nir, Phys. Rev. **D52**, 5319 (1995).

[12] M. A. Díaz et al., Phys. Rev. **D68**, 013009 (2003), hep-ph/0302021.

[13] M. Hirsch et al., Phys. Rev. **D62**, 113008 (2000), hep-ph/0004115, Err-ibid. **D65**:119901,2002.

[14] M. Hirsch and J. W. F. Valle, New J. Phys. **6**, 76 (2004), hep-ph/0405015.

[15] Atlas Technical Design Report, CERN/LHCC/99-15, ATLAS TDR 15 (1999); CMS physics: Technical Design Report, v2, CERN-LHCC-2006-021, http://cdsweb.cern.ch/record/942733, The CMS Collaboration, 2006.

[16] TESLA Technical Design Report, Part: III Physics at an e^+e^- Linear Collider, eds. R.-D. Heuer, D. Miller, F. Richard and P. Zerwas, DESY 2001-011, hep-ph/0106315; T. Abe et al. [American Linear Collider Working Group Collaboration], "Linear collider physics resource book for Snowmass 2001. 2: Higgs and supersymmetry studies," in Proc. of the APS/DPF/DPB Summer Study on the Future of Particle Physics (Snowmass 2001) , ed. N. Graf, hep-ex/0106056; K. Abe et al., JLC Roadmap Report, presented at the ACFA LC Symposium, Tsukuba, Japan 2003, http://lcdev.kek.jp/RMdraft/

[17] B. C. Allanach et al., Eur. Phys. J. **C25**, 113 (2002), hep-ph/0202233.

[18] J. A. Aguilar-Saavedra et al., Eur. Phys. J. **C46**, 43 (2006), hep-ph/0511344.

[19] M. B. Magro et al., JHEP **09**, 071 (2003), hep-ph/0304232.

[20] F. de Campos *et al.*, Phys. Rev. **D71**, 075001 (2005), hep-ph/0501153.

[21] R parity Working Group, B. Allanach *et al.*, (1999), hep-ph/9906224.

[22] R. Barbier *et al.*, (2004), hep-ph/0406039.

[23] P.-Y. Li, G.-R. Lu, J. M. Yang, H. Zhang, Eur. Phys. J. **C51**, 163 (2007), hep-ph/0608223; A. Belyaev, M.-H. Genest, C. Leroy, R. R. Mehdiyev, JHEP **0409**, 012 (2004), hep-ph/0401065; D. Choudhury, R. M. Godbole, G. Polesello, JHEP **0208**, 004 (2002), hep-ph/0207248; Yin Jun *et al*, Phys. Rev. **D65**, 116006 (2002), hep-ph/0204241; Zhou Hong *et al*, Phys. Rev. **D64**, 095006 (2001); Xi Yin *et al*, Phys. Rev. **D64**, 076006 (2001), hep-ph/0107006; B. C. Allanach *et al*, JHEP **0109**, 021 (2001), hep-ph/0106304; B. C. Allanach *et al*, JHEP **0103**, 048 (2001), hep-ph/0102173; M. Chaichian, K. Huitu, Z. H. Yu, Phys. Lett. **B490**, 87 (2000), hep-ph/0007220; G. Moreau, E. Perez, G. Polesello, Nucl. Phys. **B604**, 3 (2001), hep-ph/0003012; P. Chiappetta *et al*, Phys. Rev. **D61**, 115008 (2000), hep-ph/9910483; A. Bartl *et al*, Nucl. Phys. **B502**, 19 (1997), hep-ph/9612436.

[24] M. Hirsch and W. Porod, Phys. Rev. **D68**, 115007 (2003), hep-ph/0307364.

[25] M. Hirsch, W. Porod, J. C. Romão, and J. W. F. Valle, Phys. Rev. **D66**, 095006 (2002), hep-ph/0207334.

[26] D. Restrepo, W. Porod, and J. W. F. Valle, Phys. Rev. **D64**, 055011 (2001), hep-ph/0104040.

[27] W. Porod, M. Hirsch, J. Romão, and J. W. F. Valle, Phys. Rev. **D63**, 115004 (2001), hep-ph/0011248.

[28] J. C. Romão *et al.*, Phys. Rev. **D61**, 071703 (2000), hep-ph/9907499.

[29] B. Mukhopadhyaya, S. Roy, and F. Vissani, Phys. Lett. **B443**, 191 (1998), hep-ph/9808265.

[30] S. Y. Choi, E. J. Chun, S. K. Kang and J. S. Lee, Phys. Rev. **D60**, 075002 (1999), hep-ph/9903465.

[31] S. Borgani, A. Masiero and M. Yamaguchi, Phys. Lett. **B386**, 189 (1996), hep-ph/9605222.

[32] F. Takayama and M. Yamaguchi, Phys. Lett. **B485**, 388 (2000), hep-ph/0005214.

[33] M. Hirsch, W. Porod, and D. Restrepo, JHEP **03**, 062 (2005), hep-ph/0503059.

[34] E. J. Chun and H. B. Kim, JHEP **0610**, 082 (2006), hep-ph/0607076; K.Choi, E. J. Chun and K. Hwang, Phys. Rev. **D64**, 033006 (2001), hep-ph/0101026; E. J. Chun and H. B. Kim, Phys. Rev. **D60**, 095006 (1999), hep-ph/9906392.

[35] V. Berezinsky and J. W. F. Valle, Phys. Lett. **B318**, 360 (1993), hep-ph/9309214.

[36] M. Lattanzi and J. W. F. Valle, Phys. Rev. Lett. **99**, 121301 (2007), arXiv:0705.2406 [astro-ph].

[37] D. Aristizabal Sierra, M. Hirsch and W. Porod, JHEP **0509**, 033 (2005), hep-ph/0409241.

[38] A. Dedes, S. Rimmer and J. Rosiek, JHEP **0608**, 005 (2006), hep-ph/0603225.

[39] M. Maltoni, T. Schwetz, M. A. Tortola, and J. W. F. Valle, New J. Phys. **6**, 122 (2004), version 6 of the arXiv, hep-ph/0405172, provides results updated as of September 2007; previous works by other groups as well as the relevant experimental references are given therein.

[40] W. Porod, Comput. Phys. Commun. **153**, 275 (2003), hep-ph/0301101.

[41] T. Sjostrand *et al.*, Comput. Phys. Commun. **135**, 238 (2001), hep-ph/0010017.

[42] T. Sjostrand, Comput. Phys. Commun. **82**, 74 (1994).

[43] P. Skands *et al.*, JHEP **07**, 036 (2004), hep-ph/0311123.

[44] H. Baer, J. K. Mizukoshi, and X. Tata, Phys. Lett. **B488**, 367 (2000), hep-ph/0007073.

[45] F. de Campos *et al.*, in preparation.

[46] W. Armstrong *et al.*, CERN/LHCC , 94 (1994).

[47] D. E. Kaplan and K. Rehermann, JHEP **0710**, 056 (2007), arXiv:0705.3426 [hep-ph].

[48] Left-handed sneutrino vevs were considered in the pre–LEP days [7]. After the LEP measurements of the invisible Z-width it became clear that the existence of gauge singlet "right-handed" sneutrino vevs is necessary.

[49] Notice that displaced vertices may also arise in other scenarios of R–parity violation provided the trilinear couplings are sufficiently small; see for instance [47].

[50] A private version can be obtained sending an email to W.P.